

PHYSICS-INFORMED VIDEO DIFFUSION FOR SHALLOW WATER EQUATIONS

Yang Bai^{1,2} George Eskandar^{3*} Ziyuan Liu^{3†} Gitta Kutyniok^{1,2,4,5}

¹ Department of Mathematics, Ludwig-Maximilians-Universität München (LMU Munich), Germany

² Munich Center for Machine Learning (MCML), Munich, Germany

³ Huawei Heisenberg Research Center (Munich), Germany

⁴ Institute of Robotics and Mechatronics, DLR-German Aerospace Center, Germany

⁵ Department of Physics and Technology, University of Tromsø, Tromsø, Norway

ABSTRACT

Traditional fluid dynamics simulation pipelines combine numerical solvers with rendering, producing highly realistic results but at considerable computational cost. Diffusion-based generative video models offer a faster alternative, yet often ignore physical laws and thus fail to capture consistent dynamics. We propose a physics-informed video diffusion framework that jointly generates visual outputs and physical states. Unlike prior two-stage approaches that first simulate the physical variables and then render, we directly integrate physics constraints into the generative process, enabling simultaneous prediction of physical states and realistic videos without a separate rendering step. Built on the two-dimensional shallow water equations with terrain topography, our method produces temporally coherent water flow while maintaining physical plausibility. Experiments show that it outperforms purely data-driven video diffusion baselines in both realism and physical fidelity, while generating videos significantly faster than traditional simulation-plus-rendering pipelines.

Index Terms— Diffusion model, Physics-based simulation, Multimodal generation, Partial differential equation

1. INTRODUCTION

In traditional computer graphics (CG) pipelines, fluid visuals are generated through a two-stage process: first, a physics-based simulator computes physical states; second, these states are passed to a rendering module to produce the final images or videos. Classical solvers based on meshes or particles can reproduce complex behaviors such as turbulence, splashing, and soft-body deformation [1–6]. These simulations produce physically plausible motion. However, the additional step of photorealistic rendering for fine-scale surface details, shading, and lighting substantially increases computational costs. Consequently, producing a single high-resolution sequence can take hours or even days, making such pipelines impractical for interactive or large-scale applications.

To meet the demands of real-time graphics applications like game engines, the industry often employs spectrum-based and FFT-based water rendering techniques [7]. Instead of a physically accurate solution to the Navier-Stokes equations [8], these methods use statistical approximations. This trade-off prioritizes efficiency and visual plausibility over strict physical accuracy. In contrast, domains requiring strict physical fidelity, such as scientific research or film visual effects still rely on high-fidelity Navier-Stokes solvers. Implemented in software like Clawpack [9], OpenFOAM [10], or Basilisk [11], such solvers demand prohibitive computational resources, especially at high-grid resolutions or large scales. A range of acceleration strategies has been explored to address these challenges: for example, [12] refine low-grid resolution simulations, while Physics-Informed Neural Networks (PINNs) method [13] accelerate the solution of specific Partial Differential Equations (PDEs) terms. Nevertheless, a fundamental bottleneck persists: the combination of physics-based simulation and photorealistic rendering remains computationally expensive. The initial high cost of solving the physical equations, even when accelerated, is compounded by the subsequent time-intensive rendering process.

Recently, diffusion-based video generation methods [14, 15] have emerged as a promising alternative for dynamic scene visualization. Unlike classical pipelines, these methods synthesize video sequences directly, bypassing explicit physical simulation and costly rendering. Crucially, their generation speed is remarkably fast, depending solely on the number of sampling steps during inference, regardless of the scene’s complexity. By learning spatio-temporal patterns from large-scale datasets, they can produce visually convincing motions and textures even in complex scenarios. However, because the generated videos are not constrained by the physical laws of the real world, they frequently exhibit temporal inconsistencies and behaviors that violate basic physical principles. This limitation becomes especially pronounced for phenomena governed by complex physical equations. In such situations, especially in fluid dynamics, reproducing realistic and stable motion is extremely challenging for diffusion-based models

* : Now at Tavus.

† : Corresponding author.

without explicit physical guidance.

Contributions To address the limitations of purely data-driven video diffusion models, we propose a physics-informed video generation framework that tightly combine grid-based numerical methods with diffusion models. By embedding the initial conditions of the shallow water equations (SWEs) and terrain information into the generative pipeline, our model jointly produces video sequences and corresponding physical states. Specifically, our contributions are:

1. We present the first framework that co-generates video frames and physical states, ensuring that the generated videos adhere to the underlying fluid dynamics.
2. We incorporate the SWEs and terrain directly into the diffusion transformer, bypassing costly rendering while maintaining high visual quality, temporal stability, and physical interpretability.
3. Compared to classical simulation-plus-rendering pipelines, our method achieves over an order of magnitude reduction in runtime, with performance largely unaffected by grid resolution. Despite this speedup, it preserves between 67% to 90% of the simulation accuracy, while producing more realistic fluid motion than purely data-driven baselines, effectively bridging the gap between physical fidelity and generative efficiency.

2. RELATED WORK

2.1. Physics Enhanced Video Diffusion Models

Video diffusion models [14–17] are inherently probabilistic, and while they achieve high visual realism, adherence to physical rules is not guaranteed [18]. To improve physical consistency, several recent works [19–23] leverage large language models (LLMs) as multi-modal supervisory signals. Other works directly incorporate some physical priors: MotionCraft [24] warps the latent noise space of image diffusion models using optical flow from simulations while PhysDiff [25] iteratively projects motion onto physically plausible spaces during generation. These approaches rely on refined prompts, optical flow, or pixel-level projections as implicit physical signals to guide video generation. Although they can improve general physical plausibility, they are often insufficient for enforcing specific physical behaviors in certain scenarios. In contrast, our method explicitly embeds physical states into the video generation model, jointly producing videos and their corresponding physical quantities, which is a capability that existing video generation models cannot achieve.

2.2. Deep learning Methods for Fluid Dynamics

Machine learning has been increasingly applied to accelerate or/and improve the numerical solutions for complex fluid dynamics problems. [26] combines denoising diffusion models with PINNs, incorporating PDEs constraints during training to reduce residuals. Physics-Informed Neural Network Super-Resolution [27] integrates traditional super-resolution

techniques with physics consistency losses, preserving physical accuracy of high-grid resolution data. PirateNets [28] introduce physics-informed initialization to improve PINNs trainability and scalability, addressing derivative initialization issues. These approaches demonstrate that using deep learning to solve physical equations or integrating neural networks into traditional solvers can improve the accuracy, and scalability of PDEs solutions, or accelerate the generation of high-grid resolution physics states. However, these methods do not address the bottleneck of the time-intensive rendering required in the visualization stage.

In contrast, we are the first to address this problem by jointly integrating physics state prediction and rendering into one video diffusion model with faster inference time compared to classical rendering pipelines.

3. METHODS

In this section, we first introduce the task formulation, some SWEs preliminaries and the key components of our method.

3.1. Task Formulation

Our goal is to jointly generate a realistic N frame video $V = \{I^f\}_{f=0}^{N-1}$ and corresponding physical states $P = \{\hat{Q}^f\}_{f=0}^{N-1}$, where $I, \hat{Q} \in \mathcal{R}^{3 \times H \times W}$ given the initial image and physics conditions I^0, Q^0 , boundary conditions $D_b \in \mathcal{R}^{H \times W}$ and a text prompt D_c .

3.2. Background

Shallow Water Equations (SWEs).

The SWEs are derived from the depth-averaged Navier–Stokes equations [8], neglecting viscosity, turbulence, Coriolis and surface shear terms. They form a system of nonlinear hyperbolic PDEs [29]. In two dimensions, it can be written

$$\frac{\partial \vec{Q}}{\partial t} + \frac{\partial \vec{F}}{\partial x} + \frac{\partial \vec{G}}{\partial y} = S, \quad (1)$$

where $\vec{Q} = (h, hu, hv)^T$ denotes water height and momentum in x and y . The fluxes in the x and y directions are denoted by \vec{F} and \vec{G} , while S is the bed slope source term, which also represents the boundary condition. The river bottom is specified by a profile $S(x, y)$, where g is the gravitational constant. Expanding yields

$$\begin{aligned} \frac{\partial}{\partial t} \begin{pmatrix} h \\ hu \\ hv \end{pmatrix} + \frac{\partial}{\partial x} \begin{pmatrix} hu \\ hu^2 + \frac{1}{2}gh^2 \\ huv \end{pmatrix} \\ + \frac{\partial}{\partial y} \begin{pmatrix} hv \\ huv \\ hv^2 + \frac{1}{2}gh^2 \end{pmatrix} = \begin{pmatrix} 0 \\ -gh \frac{\partial S}{\partial x}(x, y) \\ -gh \frac{\partial S}{\partial y}(x, y) \end{pmatrix} \end{aligned} \quad (2)$$

Solutions of the SWEs may exhibit discontinuities, and evolution at cell interfaces can be interpreted as a Riemann problem [30], showing how a discontinuity propagates over time.

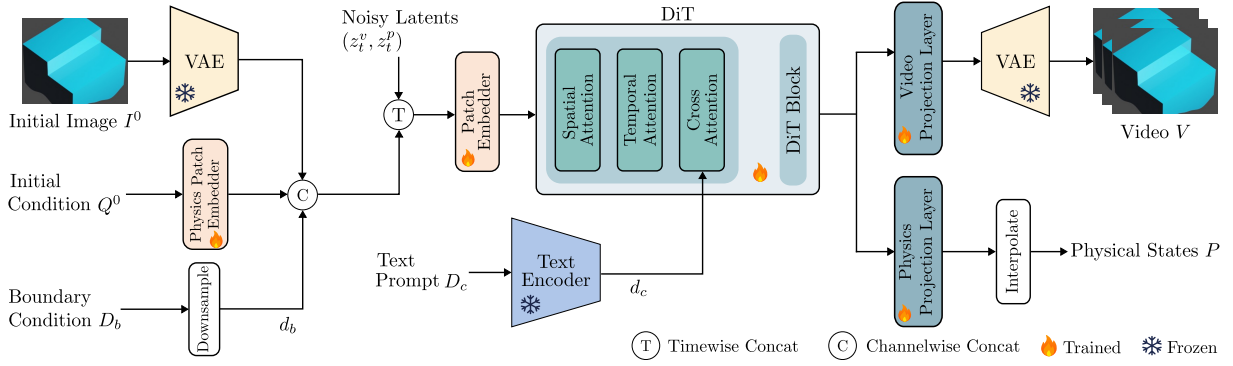


Fig. 1. Model architecture. We condition the DiT on the initial and boundary conditions (Q^0 and D_b) of the SWEs, and a rendered frame I^0 , to jointly generate the video V and physical states P .

Finite Volume Method (FVM) for Hyperbolic PDEs.

The FVM [31–33] evolves cell averages over control volumes, ensuring discrete conservation and properly handling discontinuities. On a uniform mesh, the cell average at spatial location i and time step n is

$$Q_i^n \approx \frac{1}{\Delta x} \int_{\Omega_i} Q(x, t^n) dx, \quad (3)$$

integrating over $\Omega_i \times [t^n, t^{n+1})$ gives the numerical solution

$$Q_i^{n+1} = Q_i^n - \frac{\Delta t}{\Delta x} (\bar{F}_{i+1/2}^n - \bar{F}_{i-1/2}^n), \quad (4)$$

where $\bar{F}_{i\pm 1/2}^n$ are the time-averaged numerical fluxes at cell interfaces. These fluxes are computed using Riemann solver methods such as Lax–Friedrichs, Rusanov, or Roe [30], which approximate the solution of the local Riemann problem and ensure stable propagation of waves across discontinuities.

3.3. Physics-informed video diffusion model

Model Overview. Our model is an image conditioned multi-modal Latent Diffusion Model (LDM) that generates two output modalities: the rendered video and corresponding physical states, given three input conditions: initial image and physics conditions, the boundary conditions and a text prompt. The physical states are chosen to be equal to the full time-series of FVM solutions Q_i^n of Eq. 4 at each point.

Diffusion Model Training. A pre-trained Variational Autoencoder (VAE) maps videos to latents $z_v \in \mathcal{R}^{4 \times N \times H' \times W'}$, where H' and W' are the video dimensions after the VAE downsampling. We process the physics states with a patch embedding layer to the same spatial resolution of the video latents, obtaining $z_p \in \mathcal{R}^{3 \times N \times H' \times W'}$. The boundary conditions D_b are interpolated to the latent space dimensions obtaining $d_b \in \mathcal{R}^{N \times H' \times W'}$. The text prompt is encoded with the T5 text encoder [34] to obtain a caption latent d_c . The set of input conditions is denoted by $\mathcal{C} = \{z_p^0, z_v^0, d_b, d_c\}$.

We then apply a T -step Gaussian noising process to both z_v and z_p , producing noisy video and noisy physical states z_t^v

and z_t^p that are progressively denoised by a Diffusion Transformer (DiT) network $\epsilon_\theta(\cdot, t)$. Training is performed with a joint objective $\mathcal{L}_{\text{total}} = \mathcal{L}_{\text{video}} + \mathcal{L}_{\text{phys}}$, where

$$\mathcal{L}_{\text{video}} = \mathcal{E}_{z^v, \mathcal{D}, \epsilon \sim \mathcal{N}(0,1), t} \|\epsilon - \epsilon_\theta(z_t^v, \mathcal{C}, t)\|_2^2$$

$$\mathcal{L}_{\text{phys}} = \mathcal{E}_{z^p, \mathcal{D}, \epsilon \sim \mathcal{N}(0,1), t} \|\epsilon - \epsilon_\theta(z_t^p, \mathcal{C}, t)\|_2^2$$

Model Architecture. As shown in Fig. 1, a physics embedding layer encodes the initial conditions Q^0 to the same spatial resolution as the video latent z^v . Forward diffusion is applied independently to the video and physics latents (z^v and z^p), i.e. independent noise is added to each modality. These noisy latents are then concatenated along the channel dimension with the boundary conditions d_b , ensuring that physical constraints are incorporated into the fused representation. The combined latent along with the injected prompt latents d_c , are passed through a series of DiT blocks, which perform spatio-temporal denoising while leveraging the physics-informed features. Finally, two separate Convolutional neural network (CNN)-based projection heads (P_v and P_p) map the denoised representation to the video and physics latents, respectively, allowing the model to jointly generate visually realistic video frames and physically consistent states.

4. EXPERIMENTS

To evaluate our physics-informed video diffusion model for the SWEs, we focus on its two main contributions: higher quality than normal video diffusion models and faster generation than traditional simulation-plus-rendering pipelines.

Datasets. Training and evaluation data were generated with a classical 2D Riemann solver using a second-order Roe flux from Clawpack [9] with periodic boundary conditions. Initial conditions were randomly sampled to produce 20K simulations with diverse waterbeds and 10K with a planar riverbed, each on 128×128 , 256×256 , and 512×512 grids over 1.5 seconds using TVD Runge–Kutta method [35]. And all the videos were rendered by Blender [36].

Baseline Models. We compared our method with several video generation models: CogVideoX-Fun, CogVideoX

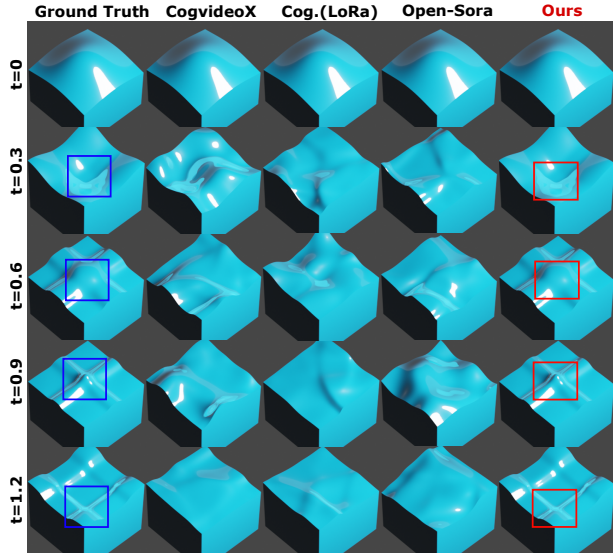


Fig. 2. Qualitative comparison of Gaussian bumps results. (I2V)-LoRA [16], and OpenSora-1.1 [17] (also can be one ablation), all fine-tuned in our dataset under comparable settings. As no previous work has addressed this combination of objectives, our experiments aim to demonstrate superior video quality compared to state-of-the-art diffusion models and faster generation than classical solvers. Therefore, other PINN-based solvers are not suitable baselines.

Ablation Study. To thoroughly evaluate our framework, we perform ablation studies with four variants: (i) naive video diffusion model without physics-informed input, and three physics-informed models using different physics patch embedding strategies for encoding physical states: (ii) linear interpolation (LI.), (iii) CNN-based embeddings, and (iv) multilayer perceptron (MLP)-based embeddings. This setup allows us to systematically investigate the impact of physics conditioning and the choice of embedding on video quality.

Implementation Details. Our physics-informed, image-conditioned video diffusion model is based on the pre-trained OpenSora-1.1 [17]. Training and inference are performed at resolutions matching the datasets, with 21 frames. Inference uses 50 sampling steps. The model is optimized using AdamW [37] for 20K steps, taking about one day on a single NVIDIA A800 GPU.

Evaluation. We evaluate on 50 test cases: 30 with random initial conditions over varying terrains, 10 planar riverbeds, 5 Gaussian bumps, and 5 classical dam-breaks. Evaluation metrics are:

- **Video Quality:** we evaluate video fidelity using LPIPS, FVD, PSNR, and SSIM against ground-truth renderings.
- **Physics Accuracy:** we compute the mean L_1 norm loss of (h, hu, hv) over all time steps against the output of the classical solver.
- **Time Consumption:** we compare total computation time between our method and the classical pipeline, where classical time includes simulation (Sim.) and rendering.

Method	LPIPS↓	SSIM↑	PSNR↑	FVD↓
CogVideoX-Fun	0.2262	0.7994	18.63	189.53
CogVideoX (I2V)-LoRA	0.2241	0.8036	18.89	178.37
Naive without Physics	0.2411	0.7862	18.28	192.64
LI. with Physics	0.1588	0.8355	22.19	137.20
MLP with Physics	0.1366	0.8423	24.91	128.69
CNN with Physics	0.1341	0.8519	25.86	125.13

Table 1. Main comparison metrics of video quality across video generation methods. Bold indicates best results. Upper: Baselines, Lower: Ablations

Resolution	Method	Time (s)			Accuracy (%)
		Sim.	Render	Total	
128×128	Classical	5.6	572	577.6	-
128×128	Ours	-	-	12	90.2
256×256	Classical	10.3	788	798.3	-
256×256	Ours	-	-	15	73.6
512×512	Classical	18.9	1463	1481.9	-
512×512	Ours	-	-	18	67.1

Table 2. Comparison of classical (Classical) pipeline, Claw-pack with Blender and our CNN with Physics method in different grid resolutions.

Discussion From Fig. 2, we observe that models without physics inputs produce nearly random wave variations, whereas our method closely matches the ground truth and accurately captures wave dynamics. This observation is further supported by Tab. 1, which shows that our method outperforms the baselines on visual metrics. The ablation results in the same table indicate that the CNN-based embedder generally outperforms both LI. and MLP-based embedders. On the other hand, Tab. 2 highlights efficiency: traditional simulation-plus-rendering pipelines see a significant increase in computation and rendering time as grid resolution rises, while our inference time remains nearly constant. One limitation of our model is the decreased accuracy of physical states as the resolution increases. Our approach can be combined with stronger video foundation models to increase the accuracy at high resolutions.

5. CONCLUSION

We proposed a physics-informed video generation framework that incorporates grid-based method into diffusion models, enabling the co-generation of videos and physical states under the SWEs. Our approach bypasses expensive rendering, yet achieves visual quality comparable to classical simulation-plus-rendering pipelines while producing results orders of magnitude faster. Compared with purely data-driven video diffusion, our method also enforces physical consistency, yielding temporally stable and interpretable outputs.

Despite these advantages, limitations remain. First, the accuracy of generated physical states degrades at higher resolutions. Second, our current work is restricted to the SWEs; extending the framework to more general governing equations, such as the Euler equations, represents an important direction for future research.

References

- [1] Jos Stam. “Stable fluids”. In: *Seminal Graphics Papers: Pushing the Boundaries, Volume 2*. 2023, pp. 779–786.
- [2] Nick Foster and Dimitri Metaxas. “Realistic animation of liquids”. In: *Graphical models and image processing* 58.5 (1996), pp. 471–483.
- [3] Nils Thürey et al. “A multiscale approach to mesh-based surface tension flows”. In: *ACM Transactions on Graphics (TOG)* 29.4 (2010), pp. 1–10.
- [4] Chris Wojtan et al. “Physics-inspired topology changes for thin fluid features”. In: *ACM Transactions on Graphics (TOG)* 29.4 (2010), pp. 1–8.
- [5] Simon Premžoe et al. “Particle-based simulation of fluids”. In: *Computer Graphics Forum*. Vol. 22. Wiley Online Library. 2003, pp. 401–410.
- [6] Barbara Solenthaler and Renato Pajarola. “Predictive-corrective incompressible SPH”. In: *ACM SIGGRAPH 2009 papers*. 2009, pp. 1–6.
- [7] Claes Johanson and Calle Lejdfors. “Real-time water rendering”. In: *Lund University* (2004).
- [8] Howard Brenner. “Navier–stokes revisited”. In: *Physica A: Statistical Mechanics and its Applications* 349.1-2 (2005), pp. 60–132.
- [9] Kyle T Mandli et al. “Clawpack: building an open source ecosystem for solving hyperbolic PDEs”. In: *PeerJ Computer Science* 2 (2016), e68.
- [10] Hrvoje Jasak. “OpenFOAM: Open source CFD in research and industry”. In: *International journal of naval architecture and ocean engineering* 1.2 (2009), pp. 89–94.
- [11] Patrick W Kenneally, Scott Piggott, and Hanspeter Schaub. “Basilisk: A flexible, scalable and modular astrodynamics simulation framework”. In: *Journal of aerospace information systems* 17.9 (2020), pp. 496–507.
- [12] Dmitrii Kochkov et al. “Machine learning–accelerated computational fluid dynamics”. In: *Proceedings of the National Academy of Sciences* 118.21 (2021), e2101784118.
- [13] Shengze Cai et al. “Physics-informed neural networks (PINNs) for fluid mechanics: A review”. In: *Acta Mechanica Sinica* 37.12 (2021), pp. 1727–1738.
- [14] Jonathan Ho et al. “Video diffusion models”. In: *Advances in neural information processing systems* 35 (2022), pp. 8633–8646.
- [15] Jonathan Ho, Ajay Jain, and Pieter Abbeel. “Denoising diffusion probabilistic models”. In: *Advances in neural information processing systems* 33 (2020), pp. 6840–6851.
- [16] Wenyi Hong et al. “CogVideo: Large-scale Pretraining for Text-to-Video Generation via Transformers”. In: *arXiv preprint arXiv:2205.15868* (2022).
- [17] Zangwei Zheng et al. “Open-sora: Democratizing efficient video production for all”. In: *arXiv preprint arXiv:2412.20404* (2024).
- [18] Saman Motamed et al. “Do generative video models understand physical principles?” In: *arXiv preprint arXiv:2501.09038* (2025).
- [19] Qinglong Cao et al. “Teaching video diffusion model with latent physical phenomenon knowledge”. In: *arXiv preprint arXiv:2411.11343* (2024).
- [20] Wang Lin et al. “Reasoning physical video generation with diffusion timestep tokens via reinforcement learning”. In: *arXiv preprint arXiv:2504.15932* (2025).
- [21] Shutao Chen et al. “DiffPhys: enhancing signal-to-noise ratio in remote photoplethysmography signal using a diffusion model approach”. In: *Bioengineering* 11.8 (2024), p. 743.
- [22] Jiayi Lv et al. “Gpt4motion: Scripting physical motions in text-to-video generation via blender-oriented gpt planning”. In: *Proceedings of the IEEE/CVF conference on computer vision and pattern recognition*. 2024, pp. 1430–1440.
- [23] Shaowei Liu et al. “Physgen: Rigid-body physics-grounded image-to-video generation”. In: *European Conference on Computer Vision*. Springer. 2024, pp. 360–378.
- [24] Antonio Montanaro et al. “Motioncraft: Physics-based zero-shot video generation”. In: *Advances in Neural Information Processing Systems* 37 (2024), pp. 123155–123181.
- [25] Ye Yuan et al. “Physdiff: Physics-guided human motion diffusion model”. In: *Proceedings of the IEEE/CVF international conference on computer vision*. 2023, pp. 16010–16021.
- [26] Jan-Hendrik Bastek, WaiChing Sun, and Dennis M Kochmann. “Physics-informed diffusion models”. In: *arXiv preprint arXiv:2403.14404* (2024).
- [27] Chulin Wang et al. “Physics-informed neural network super resolution for advection-diffusion models”. In: *arXiv preprint arXiv:2011.02519* (2020).
- [28] Sifan Wang et al. “Piratenets: Physics-informed deep learning with residual adaptive networks”. In: *Journal of Machine Learning Research* 25.402 (2024), pp. 1–51.
- [29] Peter D Lax. *Hyperbolic partial differential equations*. Vol. 14. American Mathematical Soc., 2006.
- [30] Eleuterio F Toro. *Riemann solvers and numerical methods for fluid dynamics: a practical introduction*. Springer Science & Business Media, 2013.
- [31] Robert Eymard, Thierry Gallouët, and Raphaële Herbin. “Finite volume methods”. In: *Handbook of numerical analysis* 7 (2000), pp. 713–1018.
- [32] Randall J LeVeque. *Finite volume methods for hyperbolic problems*. Vol. 31. Cambridge university press, 2002.
- [33] Eleuterio Francisco Toro et al. *Shock-capturing methods for free-surface shallow flows*. Wiley and Sons Ltd., 2001.
- [34] Colin Raffel et al. “Exploring the limits of transfer learning with a unified text-to-text transformer”. In: *Journal of machine learning research* 21.140 (2020), pp. 1–67.
- [35] Sigal Gottlieb and Chi-Wang Shu. “Total variation diminishing Runge-Kutta schemes”. In: *Mathematics of computation* 67.221 (1998), pp. 73–85.
- [36] John M Blain. *The complete guide to Blender graphics: computer modeling & animation*. AK Peters/CRC Press, 2019.
- [37] Ilya Loshchilov and Frank Hutter. “Decoupled weight decay regularization”. In: *arXiv preprint arXiv:1711.05101* (2017).